Brazilian Journal of Physics
ISSN: 0103-9733
luizno.bjp@gmail.com
Sociedade Brasileira de Física
Brasil

Rehn, J. A.; Santos, F. A. N.; Coutinho-Filho, M. D.
Combinatorial and Topological Analysis of the Ising Chain in a Field
Brazilian Journal of Physics, vol. 42, núm. 5-6, diciembre, 2012, pp. 410-421
Sociedade Brasileira de Física
Sâo Paulo, Brasil

Braz J Phys (2012) 42:410–421
DOI 10.1007/s13538-012-0108-8

STATISTICAL

Combinatorial and Topological Analysis of the Ising Chain in a Field

J. A. Rehn · F. A. N. Santos · M. D. Coutinho-Filho

Received: 11 September 2012 / Published online: 15 November 2012

Abstract We present an alternative solution of the Ising chain in a field under free and periodic boundary conditions, in the microcanonical, canonical, and grand canonical ensembles, from a unified combinatorial and topological perspective. In particular, the computation of the per-site entropy as a function of the energy unveils a residual value for critical values of the magnetic field, a phenomenon for which we provide a topological interpretation and a connection with the Fibonacci sequence. We also show that, in the thermodynamic limit, the per-site microcanonical entropy is equal to the logarithm of the per-site Euler characteristic. The canonical and grand canonical partition functions are identified as combinatorial generating functions of the microcanonical problem, which allows us to evaluate them. A detailed analysis of the magnetic field-dependent thermodynamics, including positive and negative temperatures, reveals interesting features. Finally, we emphasize that our combinatorial approach to the canonical ensemble allows exact computation of the thermally averaged value $\langle \chi \rangle$ of the Euler characteristic associated with the spin configurations of the chain, which is discontinuous at the critical fields, and whose thermal behavior is expected to determine the phase transition of the model. Indeed, our results show that the conjecture $\langle \chi \rangle (T_C) = 0$, where T_C is the critical temperature, is valid for the Ising chain.

Keywords Ising model · Combinatorics · Topology · Phase transitions

J. A. Rehn · M. D. Coutinho-Filho
Laboratório de Física Teórica e Computacional, Departamento de Física, Universidade Federal de Pernambuco, 50670-901 Recife, Pernambuco, Brazil

F. A. N. Santos (✉)
Departamento de Matemática, Universidade Federal de Pernambuco, 50670-901 Recife, Pernambuco, Brazil
e-mail: fansantos@dmat.ufpe.br

1 Introduction

In a series of papers published in the last 15 years, a topological–geometrical approach to the problem of phase transitions has been developed [1–3, 5–11]. Conjectures and theorems correlating phase transitions with topological and geometrical properties of the equipotential submanifolds in phase space have been established [8]. For a certain class of systems, very strong arguments [5–7] have suggested that a topological change of configuration space should take place during phase transitions. However, these arguments have been recently shown to fail for the ϕ^4-model [12], a finding that claims for additional investigation.

For continuous phase-space models, the topological approach to phase transitions is based on Morse theory tools [13, 14] to calculate topological invariants, such as the Euler characteristic, as functions of the energy. In particular, for proper description of the energy landscape, the critical points of the configurational energy have to be found [15]. By contrast to the attention given to continuous models, not much emphasis has been given to the application of the topological approach to discrete phase-space models, to which the classical Morse theory and the familiar methods of differential geometry are not directly applicable. Moreover, it is well known that the isolated critical points of several continuous spin models are Ising configurations [2–4, 11, 16, 17], a feature that by itself unfolds the relevance of the microcanonical approach to the Ising model.

In this work, we follow a topological approach to phase transitions that suits discrete models [18, 19], although some analogies with the continuous case are apparent. In the discrete case, the thermal average Euler characteristic was studied in the context of the canonical ensemble [18, 19] and defined through microcanonical configurations, rather than looking at the equipotential submanifolds as in the continuous case. As remarked in [18], attention to this topological quantity was already useful in the theory of percolation [21]. Here, we compute the Euler characteristic of the Ising chain in the presence of a field [22, 23], both in the context of the microcanonical and canonical ensembles. We remark that a thorough combinatorial treatment of the statistics of domains in this model has been put forward in [24], which will be useful in our treatment of the Euler characteristic in the microcanonical ensemble. In fact, combinatorics has proved very useful for a geometrical and topological characterization of the partition function in two [25] and three [26] spatial dimensions. By the same token, we will approach the one-dimensional (1-D) problem by using generating-function methods, from which the equivalence of ensembles becomes evident. This procedure will also allow us to compute the thermal average of the Euler characteristic.

This work is written as follows: in Section 2.1, we present the microcanonical solution to the Ising chain in a field, including the computation of the per-site entropy for open boundary conditions. We point out that, although the authors in [24] have not included the magnetic field contribution to the energy, their results for the multiplicity of states are equivalent to ours. In Section 2.2, we show that for ferromagnetic coupling and negative temperature, a residual per-site entropy arises for critical field values. This is verified in many variants of the Ising model, in particular for antiferromagnetic coupling and positive temperatures, including the 1-D [27, 28] and 2-D [29] cases. On the other hand, models with competing interactions also exhibit this behavior for critical values of the ratio of competing coupling constants, as studied in 1-D [30], 2-D [31], and 3-D [32] systems; a residual per-site entropy can also appear due to geometric frustration in the model, as in the well-known case of the triangular lattice [33–36], as well as in magnetic systems with the pyrochlore structure, generically called spin ice [37, 38], due to the similarity with Pauling's description of the residual entropy per site of ice [39]. Here, we present a topological interpretation for the emergence of a residual per-site entropy at the critical fields. In Section 2.3, we introduce the Euler characteristic for each microcanonical configuration of the chain, which is shown to be equal to the number of domains in the configuration. Our definition is a restriction of the one for the 2-D model [18, 19]. We also show that, in the thermodynamic limit, the logarithm of the per-site Euler characteristic is equal to the per-site entropy. In Section 3.1, we solve the canonical and grand canonical partition functions from our combinatorial solution by interpreting them as the generating function associated with the combinatorial problem for determining the microcanonical density of states. We also analyze finite-size effects on the canonical free energy under free and periodic boundary conditions. We stress that although much effort has been made to develop a combinatorial approach [25, 40] to the Onsager algebraic solution [41, 42] of the 2-D case in zero field, little attention has been devoted to this approach in the context of the Ising chain in a field, which is usually solved directly in the canonical ensemble by the transfer-matrix method [42, 43]. In order to establish the expected equivalence of ensembles, we must consider the negative-temperature range [44], as in the case of a two-level system, which happens to map on the Ising chain in zero field. In Section 3.2, the thermodynamics of the model is analyzed, and the thermally averaged per-site Euler characteristic is exactly computed. As remarked above, this quantity satisfies the expected result posed as a conjecture: $\langle\chi\rangle(T_C) = 0$, where $T_C = 0$ is the critical temperature. In Section 4, we present our concluding remarks.

2 The Microcanonical Ensemble of the Ising Chain in a Field

2.1 Combinatorial Solution

The energy functional of the Ising chain is given by

$$E(\sigma) = -J \sum_{<i,j>} \sigma_i \sigma_j - h \sum_i \sigma_i, \tag{1}$$

where the summation is over the nearest neighbor (n. n.) sites, $\sigma_i = \pm 1$ is the spin variable on site i, h is the external field, and J is the exchange interaction constant. We define the often used discrete parameters characterizing the microcanonical configurations:

$N_+(N_-)$ is the number of sites with spin $+$ $(-)$; N is the total number of sites; N_{+-} is the number of n. n. bonds with opposite spin variables. $N_{++}(N_{--})$ is the number of bonds between n. n. such that both vertexes have spins $+$ $(-)$.

Such definitions allow us to rewrite the energy as a function of fewer variables [22, 23, 43], for we have the following trivial relations: $\sum_i \sigma_i = N_+ - N_-$, and $\sum_{<i,j>} \sigma_i\sigma_j = N_{++} + N_{--} - N_{+-}$. These can be simplified by noting that the variables are not independent, since $N = N_+ + N_-$, and for periodic boundary conditions (PBC): $2N_+ = 2N_{++} + N_{+-}$, and $2N_- = 2N_{--} + N_{+-}$. Such relations are proved as follows. Imagine that we mark the bonds connecting the $+$-spin sites and count the resulting marks. We thus obtain the first equation; indeed, the left-hand side comes from the linear chain topology, since each $+$-spin site contributes twice to the total number, giving $2N_+$, while the right-hand side comes from the fact that the N_{++} bonds contribute twice to the total number of marks, giving the term $2N_{++}$, while the N_{+-} bonds contribute just once, giving N_{+-} to the total number of marks. The second equation is obtained with the same reasoning.

With free boundary conditions (FBC), we must be more careful and separate the analysis in three different cases, according to the spin variables at the beginning and the end of the chain. If both spins are $+$, since the connection between the first and last spins is not accounted for in N_{++}, we have $2N_+ = 2N_{++} + N_{+-} + 2$ and $2N_- = 2N_{--} + N_{+-}$. By the same reasoning, if both spins are $-$, we have: $2N_+ = 2N_{++} + N_{+-}$ and $2N_- = 2N_{--} + N_{+-} + 2$. Now, if the chain starts and ends with different spin species, we see that the connection between the first and last sites is not accounted for in N_{+-}, and so $2N_+ = 2N_{++} + N_{+-} + 1$ and $2N_- = 2N_{--} + N_{+-} + 1$. In summary,

$$N_{++} + N_{--} = N_+ + N_- - N_{+-}, \text{ for PBC,} \tag{2}$$

while

$$N_{++} + N_{--} = N_+ + N_- - N_{+-} - 1, \text{ for FBC.} \tag{3}$$

Let us now define the number D of domains in a given configuration of the chain as the number of maximal connected pieces of spins of the same value in the chain, i.e., without bonds between n. n. of different spins. We can relate the number of walls in the chain, N_{+-}, with its domain number: for PBC, it is clear that D is always an even number, and $N_{+-} = D$, while in the FBC case, we have that $N_{+-} = D - 1$, and D can have any parity. With such simplifications, the energy functional (1) may be written as

$$E_P(N_+, N_-, D) = -(J+h)N_+ - (J-h)N_- + 2JD \quad \text{(for PBC)}, \tag{4}$$

while

$$E_F(N_+, N_-, D) = E_P(N_+, N_-, D) - J \quad \text{(for FBC)}. \tag{5}$$

These expressions are important because they clearly identify the combinatorial problem we are concerned with. By keeping constant the variables in these expressions, we can enumerate the degeneracy of a level with energy E, i.e., its thermodynamical weight $W(E)$, which leads to the microcanonical ensemble solution.

We shall separate the study of the microcanonical solution in two parts, according to the parity of the number of domains. For PBC, we always have that $D = 2k$, $k \in \mathbb{N}$, which is the case for FBC only if the chain extremities have different spin species; in fact, by closing the chain extremities in the referred FBC case, we map onto $2k$ domains under PBC. On the other hand, under FBC, if the chain extremities have the same spin species, we have $2k + 1$ domains, which are mapped onto $2k$ domains under PBC when we close the chain extremities.

Given this explanation on the connection between the parity of the number of domains and boundary conditions, we shall carry out the solution for the FBC case, knowing from the above reasoning that the multiplicity of states for fixed values of N_+, N_- and D, also covers the PBC case. We thus want to solve the combinatorial problem of determining how many distinct configurations exist, under fixed N, N_+, and D. This was done first by Ising [22, 23] and more recently, in the context of the statistics of domains, by Denisov and Hanggi [24]. Here, we present a similar procedure to solve the combinatorial problem and use the result to calculate the per-site entropy, its residual value for critical fields, and the average Euler characteristic over microcanonical spin configurations. Consider first the case $D = 2k$; then, $N_+ \geq k = D/2$ and $N_- = N - N_+ \geq k = D/2$. Under these conditions, our combinatorial problem reduces to analyzing the number of different solutions for the following system of two equations in nonnegative integer variables, each variable being the number of spins in domain j:

$$\begin{cases} u_1 + \ldots + u_k = N_+ - k, \\ d_1 + \ldots + d_k = N_- - k = N - N_+ - k, \end{cases} \tag{6}$$

where $u_j + 1, d_j + 1 \in \mathbb{N} \cup \{0\}, \forall j$, represent the number of + and − spins in the j-th domain, respectively. The number of different solutions is simply

$$l = \binom{N_+ - 1}{k - 1}\binom{N_- - 1}{k - 1}\Theta\left(N_+ - \frac{D}{2}\right) \times \Theta\left(N - N_+ - \frac{D}{2}\right), \tag{7}$$

but since we have an extra degeneracy given by the spin value (+ or −) in the leftmost domain in the chain, the total number of configurations is

$$W_{\rm even} = 2l = 2\binom{N_+ - 1}{k - 1}\binom{N_- - 1}{k - 1}\Theta\left(N_+ - \frac{D}{2}\right) \times \Theta\left(N - N_+ - \frac{D}{2}\right). \tag{8}$$

Consider now the case $D = 2k + 1$. Then, according to our previous reasoning, we must have the same spin values at both extremities, so that we have two possibilities: $k + 1$ domains of spin + and k of spin −, or vice versa. In the first situation, we have the constraints $N_+ \geq k + 1 = (D + 1)/2$ and $N_- = N - N_+ \geq k = (D - 1)/2$, while for the other possibility, $N_+ \geq k = (D - 1)/2$ and $N_- = N - N_+ \geq k + 1 = (D + 1)/2$. In the first case, the problem of finding the degeneracy of the configurations is equivalent to that of finding the number of solutions for a system of equations similar to (6), with $k \to k + 1$ only in the first equation. The multiplicity of states for an odd number of domains is therefore

$$W_\pm = \binom{N_\pm - 1}{k}\binom{N_\mp - 1}{k - 1}\Theta\left(N_+ - \frac{D \pm 1}{2}\right) \times \Theta\left(N - N_+ - \frac{D \mp 1}{2}\right), \tag{9}$$

which implies that

$$W_{\rm odd} = W_+ + W_-. \tag{10}$$

It is easily verified that the previous microcanonical solution sums up to give the total expected number of possible configurations for a chain of size N, i.e., 2^N. To this end, we first recall the identity

$$\sum_{m=k}^{n-k}\binom{m}{k}\binom{n - m}{k} = \binom{n + 1}{2k + 1}. \tag{11}$$

Next, we add the degeneracies $W_{\rm even}$ and $W_{\rm odd}$, given by (8) and (9–10) over the numbers of spins allowed by the Heaviside functions on the right-hand sides of (8) and (9) to obtain the following results for even and for odd number of domains

$$\sum_{N_+=k}^{N-k} W_{\rm even} = 2\binom{N - 1}{2k - 1} = 2\binom{N - 1}{D - 1}, \tag{12}$$

and

$$\sum_{N_+} W_{\rm odd} = \sum_{N_+=k+1}^{N-k} W_+ + \sum_{N_+=k}^{N-k-1} W_- = 2\binom{N - 1}{2k} = 2\binom{N - 1}{D - 1}. \tag{13}$$

respectively. As a side remark, we notice that the above Ising density of states corresponds to the density of isolated critical points of the 1-D XY model in the zero field limit [4, 8].

Finally, we sum over the number of domains to obtain the expected total number of microstates:

$$\sum_{D=1}^{N} 2\binom{N - 1}{D - 1} = 2^N. \tag{14}$$

The derived multiplicity of states $W_{\rm even}$ and $W_{\rm odd}$ in (8) and in (9) and (10), respectively, can now be used to compute the per-site entropy as a function of the per-site energy of the chain under the appropriate boundary condition, i.e., $E = E_F(N_+, N_-, D)$ for FBC, or $E = E_P(N_+, N_-, D)$ for PBC:

$$\frac{S_{P,F}(E/N)}{N} = \frac{k}{N}\ln\left[\sum_{\substack{N_+, D \\ E_{P,F}(N_+, N_-, D) = E}} (W_{\rm odd} + W_{\rm even})\right]. \tag{15}$$

For simplicity, we henceforth set $k \equiv 1$.

We note that the pigeonhole principle imposes the restrictions $d/2 \leq n_+ \leq 1 - d/2$, where $d = \lim_{N\to\infty} D/N$, and $n_+ = \lim_{N\to\infty} N_+/N$, as explicitly shown for finite N by the Heaviside functions on the right-hand sides of (8) and (9). Since the energy can be written as a function of n_+ and d, we can represent the configuration space as the two-dimensional space n_+ vs. d. The inequalities $d/2 \leq n_+ \leq 1 - d/2$ then restrict the allowed spin configurations to region inside the triangle in Fig. 1 (note that on the line $d = 0$ only the points $n_+ = 0$ and $n_+ = 1$ belong to this domain).

In order to compute the per-site entropy from (15), we must therefore sum the microstates corresponding to points inside the triangle in Fig. 1 over isoenergetic

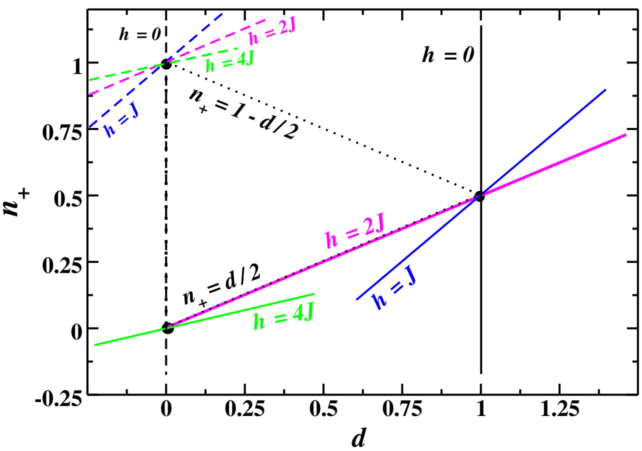

Fig. 1 (Color online) Region of allowed per-site numbers of + spins and domains associated with the multiplicity of microstates in the thermodynamic limit. The *dashed solid lines* show the minimum (maximum) energies for various magnetic fields

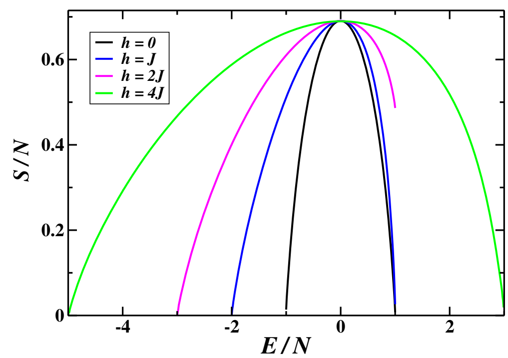

Fig. 2 (Color online) Per-site entropy as a function of the per-site energy for $N = 1{,}000$, $J = 1$, $\delta(E/N) = 0.005$ under FBC for various magnetic field values

levels. Note also that the range of allowed per-site energies $e = E/N$ is derived from (5): if $J > 0, h > 0$, the minimum energy is $e_{\min} = -(h + J)$, with $n_+ = N_+/N = 1$ and $d = D/N = 1/N \to 0$, as illustrated by the dashed lines in Fig. 1 for a few values of h. The maximum energy level is $e_{\max} = J$, with $n_+ = 1/2$ and $d = 1$, if $h \leq 2J$, or $e_{\max} = h - J$, with $n_+ = 0$ and $d \to 0$, if $h \geq 2J$, as illustrated in by the solid lines in Fig. 1 for a few values of h. These results are exact in the thermodynamic limit, with additive corrections of $O(1/N)$.

For negative magnetic field h (and $J > 0$), the results are completely analogous, and we infer that the field can induce qualitative changes in the magnetic behavior of the chain: indeed, the maximum energy is attained for antiferromagnetic configurations if $|h| < 2J$, while it is attained for ferromagnetic configurations if $|h| > 2J$.

We now proceed to describing the numerical computation of (15) under FBC, with $J = 1$ and $N = 1,000$. For fixed e, we vary the discrete parameters N_+, D and check if the corresponding energy $e_F = E_F(N_+, N_-, D)/N$, given by (5), lies within the interval $(e - \delta e, e + \delta e)$, where we have chosen $\delta e = 0.005$. If it does, we sum the corresponding multiplicity of states given by (8), for even D, or by (9, 10), for odd D. The total sum of all the possible multiplicity of states in the energy neighborhood $(e - \delta e, e + \delta e)$ is the thermodynamic weight of the per-site entropy in (15), which is plotted in Fig. 2 for various magnetic fields. We notice that the transfer-matrix method has been used to numerically compute such entropy curves for small N [45].

In the high-energy branches of Fig. 2, i.e., the $E/N > 0$ branches, the per-site entropy decreases with energy and is, hence, in the negative range of temperatures, as follows from the relation $\frac{1}{T} = \partial S/\partial E$. Therefore, we identify $T = 0+ \equiv 0$ ($T = 0-$) with the minimum (maximum) energy. Notice, however, that negative-temperature states correspond to positive-temperature states with reversed signs for J and h. Indeed, inspection of (1) explicitly shows that the Boltzmann factor $\exp(-\beta E)$ and, therefore, the partition function remain invariant under simultaneous reversal of the signs of T, J, and h (since we are dealing with a model with bounded allowed energy states, negative temperatures do not lead to problems with the convergence of the partition function). The high-energy states for $J > 0$ correspond therefore to low-energy states with $J < 0$. In fact, the observed residual per-site entropy in Fig. 2, for the critical field $h = 2J$, corresponds to the well-known residual per-site entropy for an antiferromagnetic Ising chain in the positive-temperature regime [27, 28].

2.2 Residual per-site Entropy at $h = \pm 2J$

As can be seen from (4), the per-site energy in the Ising chain for given chain size, external magnetic field, and coupling constant is determined by the two parameters $n_+ = N_+/N$ and $d = D/N$. If e is the per-site energy in the thermodynamic limit, we have from (4) that

$$e = -2hn_+ + 2Jd - (J - h). \tag{16}$$

Notice that a fixed e value defines a straight line with slope J/h in Fig. 1; the allowed states are inside the triangle in the figure. Changing the energy, at fixed ratio J/h, corresponds to translating that line. Furthermore, the entropy is obtained as a function of energy by taking the logarithm of the total multiplicity of states lying on the overlap of such lines with the region of allowed microscopic states. A similar perspective on the 2-D

Ising microstates in magnetization vs. energy space has been presented in [46].

From this perspective, we can understand the plots in Fig. 2, which show the per-site entropy as a function of energy for various magnetic fields. For magnetic fields different from $\pm 2J$, the contribution of each isoenergetic line to the total multiplicity of states per site becomes arbitrarily small at the points of minimum ($T = 0$) and maximum ($T = 0-$) energy, since the lines pass through the corners of the triangle in Fig. 3, which displays only positive fields because the energy in (16) is invariant under the simultaneous transformations $n_+ \leftrightarrow 1/2 - n_+$, $h \leftrightarrow -h$, so that the negative-field plots are symmetric to the ones in the figure with respect to the line $n_+ = 1/2$.

For $h = \pm 2J$, special behavior emerges when the energy is maximum, since the isoenergetic lines now coincide with the nonvertical edges of the triangle. In fact, the associated multiplicity of states is exponentially large and gives rise to a residual per-site entropy. We therefore witness a topological change at the critical field: as shown by the middle panel in Fig. 3, the set representing the overlap between the domain of available macroscopic states and the straight line representing maximum energy have nonzero measure at $h = 2J$, exactly.

Interestingly, the multiplicity of states at the two nonvertical sides of the triangle is exactly the $(N+2)$-th term of the Fibonacci sequence, and, therefore, the residual per-site entropy for such a magnetic field at the maximum energy is exactly equal to the logarithm of the golden ratio. A simple way to see why the multiplicity of states in this specific situation is given by the terms in the Fibonacci sequence is to search for the configurations of the chain maximizing the energy at $h = 2J$ and $E = J(-4N_+ + 2D + N)$.

To this end, first notice that $2J$ is exactly the energy of a spin with two nearest neighbors of opposite spin. The maximum energy $E = NJ$ for $h = 2J$ is therefore attained by those configurations in which all spins are $-$ (more generally, antiparallel to the field), except for some isolated sites where the spins are $+$ (i.e., parallel to the field). For simplicity, assume FBC and let us call $f(N)$ the total number of configurations of N spins in a chain in which the $+$ spins are isolated from all other $+$ spins. It is then a simple matter to construct a recursive relation: if the leftmost spin is not $+$, there are $f(N-1)$ ways to organize the remainder of the chain; if it is $+$, there are $f(N-2)$ ways to organize the remainder, and therefore

$$f(N) = f(N-1) + f(N-2) \tag{17}$$

Since $f(1) = 2$ and $f(2) = 3$, we see that $f(N)$ will be the $(N+2)$-th term in the Fibonacci sequence.

It is worth noticing that the residual per-site entropy at the critical fields in the simple case of an Ising chain can put in correspondence with the residual entropies of more general models. A decimation transformation of decorated Ising models can map them to the simple Ising chain under study here; by imposing the conditions $h^* = \pm 2J^*$ on the effective coupling constant $J^*(T, h)$ and the effective magnetic field $h^*(T, h)$, we then obtain curves in the $T - h$ plane along which the system has a residual per-site entropy. This is the case, e.g., of the AB_2 Ising chain in a field [47], for which the decimation of the B sites maps the model onto a linear Ising chain in an effective field with an effective coupling between the A sites.

2.3 Euler Characteristic

Blanchard et al. [18] offers a very simple definition for the Euler characteristic in one dimension: given a configuration of the chain, the Euler characteristic χ_+ (χ_-) associated with spin-+ ($-$) sites is defined as the Euler characteristic of the graph whose vertex set is constituted of spin-+ ($-$) sites, and whose edge set is constituted of the bonds of n. n. with spin $+$ ($-$) vertex. We, thus, have that $\chi_+ = N_+ - N_{++}$ ($\chi_- = N_- - N_{--}$), and (2) and (3) yield $\chi_+ = N_{+-}/2 = D/2$ ($\chi_- =$

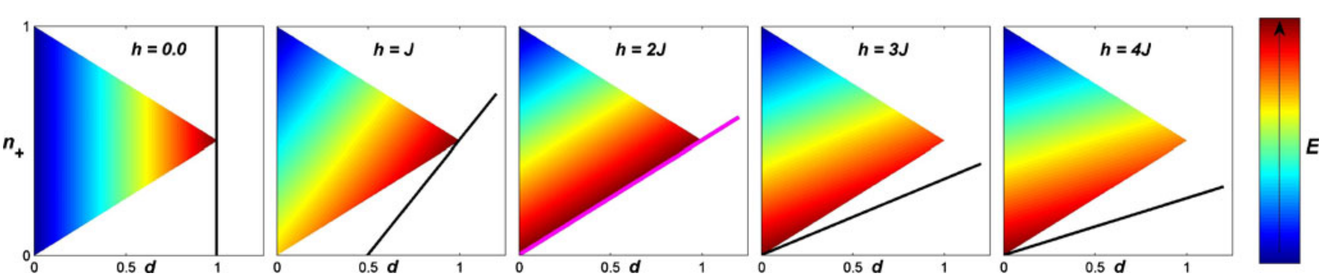

Fig. 3 (Color online) Energy contour maps for various magnetic fields in configuration (n_+ vs. d) space. For each panel, a *solid line* shows the maximum energy isoenergetic. For $h = 2J$ (central panel), the *straight line* overlaps the lower edge of the allowed states triangle

$N_{+-}/2 = D/2$) for PBC, while for FBC, we have three cases to consider, depending on the spin variables at the chain extremities: $\chi_+ = (D+1)/2$ ($\chi_- = (D-1)/2$), when both are $+$ spins, $\chi_+ = (D-1)/2$ ($\chi_- = \frac{D+1}{2}$), when both are $-$, and $\chi_+ = \frac{D}{2}$ ($\chi_- = \frac{D}{2}$), when they are different. In view of the resulting complementary behavior for the Euler characteristic with respect to $+$ and $-$ sites, we simply define the Euler characteristic of the chain as the sum $\chi = \chi_+ + \chi_- = D$, equivalent to the number of domains in all cases. The Euler characteristic of the Ising chain as a function of its per-site energy can therefore be obtained in the microcanonical distribution from the following prescription

$$\chi_{(\text{Ising})}(E/N) = \sum_{\substack{N_+,D \\ E_{F;P}(N_+,N_-,D)=E}} D(W_{\text{odd}} + W_{\text{even}}). \tag{18}$$

The sum over N_+ is given by (12) and (13), whereas the sum over D is formally performed by using the restriction on the fixed energy value. It follows that

$$\chi_{(\text{Ising})}(E/N) = 2D\binom{N-1}{D-1}. \tag{19}$$

Therefore, since $0 \leq D/N \leq 1$, we have that

$$\lim_{N\to\infty} \frac{\ln(\chi_{(\text{Ising})})}{N} = \lim_{N\to\infty} \frac{S_{\text{Ising}}}{N}, \tag{20}$$

in agreement with the numerics in Fig. 2 for the per-site entropy.

Equation (19) yields an interesting illustration of the relation between the topological approaches for phase transitions in models with discrete [18, 19] or continuous [8] symmetries, in the context of a comparative discussion of the Ising chain and the 1-D XY model. The Euler characteristic for the latter model in the zero field limit, $\chi_{(XY)}$, is given by [4]

$$|\chi_{(XY)}| = 2\binom{N-2}{n_d}, \tag{21}$$

where n_d is the number of domain walls, and a domain is defined as a set of contiguous pieces of the chain in which all angles, associated with the isolated critical points of the model [2, 3], are 0 or π. We thus get that, in zero field, $\lim_{N\to\infty} \frac{\ln(|\chi_{(XY)}|)}{N} = \lim_{N\to\infty} \frac{\ln(\chi_{(\text{Ising})})}{N} = \lim_{N\to\infty} \frac{S_{\text{Ising}}}{N}$, apart from the arbitrariness in the choice of the coupling constant and zero energy level. We also recall that the connection between discrete and continuous models has been extensively exploited in the contexts of statistical mechanics, the renormalization group description of critical phenomena [48], and quantum field theory [49].

3 Equivalence of Ensembles for the Ising Chain in a Field

3.1 Combinatorial Solution

We now turn to showing that the microcanonical, canonical, and grand canonical ensembles yield equivalent results. To this end, we first notice that the generating function associated with the combinatorial problem of determining the microcanonical distribution can be identified with the canonical partition function of the model:

$$Z_P(N; a, u, d) = \sum_{N_+,N_-,D} W_P(N_+, N_-, D) a^D u^{N_+} d^{N_-}; \tag{22}$$

$$e^{-\beta J} Z_F(N; a, u, d) = \sum_{N_+,N_-,D} W_F(N_+, N_-, D) a^D u^{N_+} d^{N_-}. \tag{23}$$

Indeed, given the definition

$$Z_{P,F} = \sum_{N_+,N_-,D} W_{P,F}(N_+, N_-, D) e^{-\beta E_{P,F}(N_+,N_-,D)}, \tag{24}$$

and (4, 5), we see that

$$a = e^{-2\beta J}, \quad u = e^{\beta(J+h)}, \quad \text{and} \quad d = e^{\beta(J-h)}. \tag{25}$$

We have thus provided a combinatorial interpretation for the Laplace transform, (24), relating the canonical and microcanonical ensembles, in agreement with general prescriptions of statistical mechanics. Next, we try to compute the above sums by examining the underlying combinatorial problem in light of the theory of enumerating generating functions [50] and recalling that Ising [22, 23] was able to carry out the sum in (23) by comparing the exact form of the power series with the expansion of the grand canonical partition function in powers of the fugacity $z = e^{\beta\mu}$, whose coefficients are the canonical partition functions for different chain sizes. Below, at a certain stage of our procedure, we shall also compute the grand canonical partition function.

Let us start out by analyzing the microcanonical ensemble from a generating-function viewpoint. We introduce artificial variables x_i to keep track of the number chain sites inside the i-th domain, the power $x_i^{s_i}$

indicating that the i-th domain contains s_i chain sites. Therefore, the function

$$f(x_1, ..., x_{2k}) = \left(x_1 + x_1^2 + ...\right) ... \left(x_{2k} + x_{2k}^2 + ...\right) = \frac{x_1 ... x_{2k}}{(1 - x_1) ... (1 - x_{2k})}, \quad (26)$$

combines all the possible terms $x_1^{s_1} ... x_{2k}^{s_{2k}}$, with $s_i \geq 1$, i.e., all the ways of constructing chains with s_i sites inside domain i.

For the Ising chain, we can see that by imposing $x_{2j-1} = u$ and $x_{2j} = d$, for $1 \leq j \leq k$, the coefficient of the term $u^{N_+} d^{N_-}$ in the function $g'_k(u, d) \equiv f(u, d, \ldots, u, d)$ tells us the number of ways of placing N_+ spins $+$ in k domains and N_- spins $-$ in k domains, with the leftmost domain of a fixed spin value, either $+$ or $-$. To account for the two possibilities for the leftmost domain ($+$ or $-$), we simply must include an extra multiplicative factor 2 in our generating function:

$$g_k^{(I)}(u, d) = 2 g_k^{'(I)}(u, d) = \frac{2u^k d^k}{(1 - u)^k (1 - d)^k}, \quad (27)$$

the power series expansion of which generates a coefficient associated with each terms $u^{N_+} d^{N_-}$.

The coefficients, denoted $\left[u^{N_+} d^{N_-}\right] g_k^{(I)}(u, d)$, can be identified with the microcanonical distribution W_{even} in (8):

$$\left[u^{N_+} d^{N_-}\right] g_k^{(I)}(u, d) = 2 \binom{N_+ - 1}{k - 1} \binom{N_- - 1}{k - 1}. \quad (28)$$

We have also to account for the possibility of having the two extremities of the chain with sites of the same domain type, since these possible configurations are not counted in the above generating function. We therefore define

$$f_{2k+1}(x_1, ..., x_{2k+1}) = \left(x_1 + x_1^2 + ...\right) ... \left(x_{2k+1} + x_{2k+1}^2 + ...\right) = \frac{x_1 ... x_{2k+1}}{(1 - x_1) ... (1 - x_{2k+1})}, \quad (29)$$

with $x_{2j-1} = u$, for $1 \leq j \leq k + 1$, and $x_{2j} = d$, for $1 \leq j \leq k$, thus obtaining $g_k^{(II)}(u, d) \equiv f_{2k+1}(u, d, \ldots, u, d, u)$. Alternatively, we can impose that $x_{2j-1} = d$, for $1 \leq j \leq k + 1$, and $x_{2j} = u$, for $1 \leq j \leq k$, which implies $g_k^{(III)}(u, d) \equiv f_{2k+1}(d, u, \ldots, d, u, d)$. Therefore, the microcanonical distributions $W_\pm$ in (9) are recovered:

$$\left[u^{N_+} d^{N_-}\right] g_k^{(i)}(u, d) = \binom{N_\pm - 1}{k} \binom{N_\mp - 1}{k - 1} \quad (i = II, III). \quad (30)$$

We shall now allow for all possible domain numbers. In doing so, we must treat separately the PBC and FBC cases: for FBC, the coefficients (II) and (III) above are associated with spin configurations containing one domain more than the configurations related to the coefficient (I); while, for PBC, all three coefficients are associated with configurations with the same domain number. We introduce the definitions

$$\Xi_F^{(I)}(a, u, d) = \sum_{k=1}^{\infty} g_k^{(I)}(u, d) a^{2k} = \frac{2\alpha\gamma}{1 - \alpha\gamma} = \alpha\gamma\, \Xi_P^{(I)}(a, u, d); \quad (31)$$

$$\Xi_F^{(i)}(a, u, d) = \sum_{k=0}^{\infty} g_k^{(i)}(u, d) a^{2k+1} = \frac{\alpha_{(i)}}{1 - \alpha\gamma} = a\, \Xi_P^{(i)}(a, u, d), \quad i = II, III, \quad (32)$$

where $\alpha_{(II)} = \alpha = \dfrac{au}{1 - u}$ and $\alpha_{(III)} = \gamma = \dfrac{ad}{1 - d}$.

On the other hand, the combinatorial problem subject to the condition that the chain have a specified size $N = N_+ + N_-$ can be obtained from the series expansions of the three contributions to the grand canonical partition functions $\Xi_{P,F}^{(I),(II),(III)}(a, zu, zd)$ in powers of the fugacity $z = e^{\beta\mu}$:

$$\Xi_{P,F}^{(I),(II),(III)}(a, zu, zd) = \sum_{N=0}^{\infty} Z_{P,F}^{(I),(II),(III)}(N; a, u, d) z^N, \quad (33)$$

where $Z_{P,F}^{(I),(II),(III)}(N, a, u, d)$ are the three contributions for the canonical partition functions for chains of N sites and FBC or PBC.

We now let $u, d \to zu, zd$ in (31) and (32) and define $p(z) = 1 - (u + d)z + ud(1 - a^2)z^2$ to obtain expressions for the grand canonical partition functions with FBC [22] and PBC,

$$\Xi_F = \frac{a(u + d)z + 2aud(a - 1)z^2}{p(z)} \quad \text{and}$$

$$\Xi_P = \frac{2 - (u + d)z}{p(z)}, \quad (34)$$

respectively.

Next, we discuss the main steps leading to the canonical partition functions in (33). First, note that $p(z)$ is such that $p(z) = (z - \lambda_1)(z - \lambda_2) ud(1 - a^2)$, with

$$\lambda_{1,2} = \frac{1}{ud(1 - a^2)} \left[\frac{(u + d)}{2} \pm \frac{1}{2}\sqrt{(u - d)^2 + 4uda^2}\right] = \lambda_1 \lambda_2 \sigma_\pm, \quad (35)$$

and

$$\sigma_\pm = \frac{(u + d)}{2} \pm \frac{1}{2}\sqrt{(u - d)^2 + 4uda^2}. \quad (36)$$

Substitution of the right-hand sides in (25) for a, u, and d shows that these are the exact expressions for the eigenvalues of the transfer matrix for the Ising chain in a field.

Using the polynomial roots in (35) and (36) and expanding $p(z)^{-1}$ in (34) in a geometric series, we find for the FBC case that

$$\Xi_F(a, zu, zd) = \frac{a(u+d)z + 2aud(a-1)z^2}{ud(1-a^2)} \frac{1}{\lambda_1\lambda_2} \times \left[\sum_{i=0}^{\infty}\left(\frac{z}{\lambda_1}\right)^i\right]\left[\sum_{i=0}^{\infty}\left(\frac{z}{\lambda_2}\right)^i\right]. \quad (37)$$

Here, the coefficient of z^N has the form

$$\left[z^N\right] \Xi_F(a, zu, zd) = 2aud(a-1)\Lambda^{(N-1)} + a(u+d)\Lambda^{(N)}, \quad (38)$$

where we have used that

$$\frac{1}{\lambda_2^q} - \frac{1}{\lambda_1^q} = \frac{\lambda_1^q - \lambda_2^q}{(\lambda_1\lambda_2)^q} = \sigma_+^q - \sigma_-^q, \ \forall q \in \mathbb{N}; \quad (39)$$

$$\Lambda^{(N)} = \frac{\sigma_+^N - \sigma_-^N}{\sigma_+ - \sigma_-}. \quad (40)$$

A similar analysis of the periodic case leads to the result

$$Z_P(N; a, u, d) = 2\Lambda^{(N+1)} - \left[2(u+d) + a(u^2+d^2)\right]\Lambda^{(N)} + ud\left[2 - a(u+d)\right]\Lambda^{(N-1)}. \quad (41)$$

Substitution of (25) into (38) and (41) followed by some algebra then leads to the equalities

$$Z_F = e^{\beta J}\left(\frac{\sigma_+^N}{\sigma_+ - \sigma_-} e^{-2\beta J}\left(\sigma_+ - \tanh(\beta J)\sigma_-\right) + \frac{\sigma_-^N}{\sigma_+ - \sigma_-} e^{-2\beta J}\left(\tanh(\beta J)\sigma_+ - \sigma_-\right)\right); \quad (42)$$

$$Z_P = \sigma_+^N + \sigma_-^N; \quad (43)$$

$$\sigma_\pm = e^{\beta J}\left(\cosh(\beta h) \pm \sqrt{\sinh^2(\beta h) + e^{-4\beta J}}\right), \quad (44)$$

Equations (42) and (44) and (43) and (44) agree with the canonical partition function expressions for FBC [22] and PBC [43], respectively. This concludes our alternative combinatorial solution for the ensembles associated with the Ising chain, under free and periodic boundary conditions.

From the above expressions for the canonical partition functions, we get the per-site Gibbs free energy of the system:

$$g_{P,F} = G_{P,F}/N = -T\ln(Z_{P,F})/N, \quad (45)$$

which allows us to identify distinct finite-size effects due to the different boundary conditions. It can be easily seen that both cases have the same thermodynamic limit, namely,

$$g_\infty = \lim_{N\to\infty} G_{P,F}/N = -T\ln(\sigma_+). \quad (46)$$

The finite-size corrections to the free energy for PBC are

$$N\left[g_P(N) - g_\infty\right] = -T\sum_{j=1}^{\infty}(-1)^{j-1}\frac{1}{j}\left(\frac{\sigma_-}{\sigma_+}\right)^{Nj}, \quad (47)$$

while for FBC, we have that

$$N\left[g_F(N) - g_\infty\right] = -J - T\ln(A) - T\sum_{j=1}^{\infty}(-1)^{j-1}\frac{1}{j}B^j\left(\frac{\sigma_-}{\sigma_+}\right)^{Nj}, \quad (48)$$

where

$$A = \frac{a}{\sigma_+ - \sigma_-}\left(\sigma_+ - \frac{1-a}{1+a}\sigma_-\right) = {}^{-2\beta J}\frac{\sigma_+ - \tanh(\beta J)\sigma_-}{\sigma_+ - \sigma_-}; \quad (49)$$

$$B = \frac{\frac{1-a}{1+a}\sigma_+ - \sigma_-}{\sigma_+ - \frac{1-a}{1+a}\sigma_-} = \frac{\tanh(\beta J)\sigma_+ - \sigma_-}{\sigma_+ - \tanh(\beta J)\sigma_-}. \quad (50)$$

Since $\sigma_-/\sigma_+ < 1$, we can see that for very large N the first term in each series is dominant. We therefore have the asymptotic behaviors

$$N\left[g_P(N) - g_\infty\right] = -T^{-N/\xi} \quad \text{(PBC)} \quad (51)$$

$$N\left[g_F(N) - g_\infty\right] = -J - T\ln(A) - TB^{-N/\xi} \quad \text{(FBC)}. \quad (52)$$

Here, we have introduced the *correlation length* of the model [51]:

$$\xi = \left[\ln\left(\frac{\sigma_+}{\sigma_-}\right)\right]^{-1}, \quad (53)$$

which shows that the correction for PBC is exponential, while a power law correction $\frac{1}{N}$ is clearly identified for FBC.

3.2 Thermodynamics, Euler Characteristic, and Phase Transition

The per-site Gibbs free energy in the thermodynamic limit, (46), determines the thermodynamic functions for the model, such as the per-site energy, entropy, and magnetization. The closed expressions for these quantities in the thermodynamic limit are

$$e = \frac{\partial (g_\infty / T)}{\partial \beta} = -J - h\frac{2e^{\beta J}\sinh(\beta h)}{\sigma_+ - \sigma_-} + 2J\frac{2e^{-2\beta J}}{\sigma_+(\sigma_+ - \sigma_-)}; \quad (54)$$

$$s = -\frac{\partial g_\infty}{\partial T} = k\ln(\sigma_+) + k\beta e; \quad (55)$$

and

$$m = -\frac{\partial g_\infty}{\partial h} = \frac{2e^{\beta J}\sinh(\beta h)}{\sigma_+ - \sigma_-}, \quad (56)$$

respectively.

While e and s are even functions of h, the magnetization m is an odd function. The three thermodynamic functions are shown in Figs. 4, 5, and 6, for fixed $J = 1 > 0$ and various nonnegative fields h.

As Fig. 5 shows, and in agreement with our discussion in Section 2, the maximum per-site energy at $T = 0^-$ is J for $|h| \leq 2J$ and $(|h| - J)$ for $|h| > 2J$, which correspond to antiferromagnetic and ferromagnetic spin configurations, respectively. On the other hand, the per-site entropy in Fig. 5 displays no loss of continuity as a function of temperature except at the critical fields $h = \pm 2J$, where the residual per-site entropy is the logarithm of the golden ratio $\phi = \frac{1+\sqrt{5}}{2}$. We also emphasize that the per-site entropy is always a convex function of the temperature, showing the stability of states for any magnetic field and temperature.

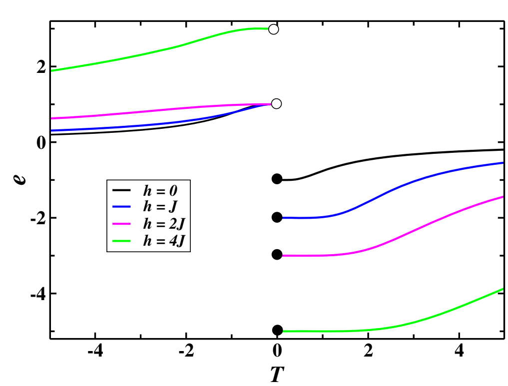

Fig. 4 (Color online) Per-site energy in the thermodynamic limit as a function of the temperature for the indicated magnetic fields

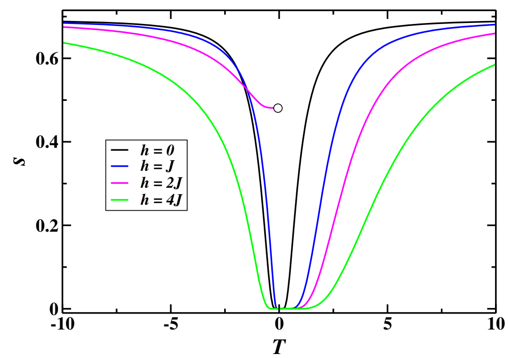

Fig. 5 (Color online) Per-site entropy in the thermodynamic limit as a function of the temperature for the indicated magnetic fields

Moreover, the per-site magnetization as a function of temperature in Fig. 6 deviates from its usual monotonic behavior for $|h| < 2J$ and approaches the antiferromagnetic state as $T \to 0^-$. At the critical fields $\pm 2J$, it takes the values $\mp 1/\sqrt{5}$. Notice also that in zero field, the per-site magnetization is zero for any $T \neq 0$; at the critical temperature $T_C = 0$, however, two values become possible: ± 1, indicated by the filled circles in the figure and associated with the long-range order in the chain. The above-mentioned results are valid for $J > 0$, while for $J < 0$, the corresponding ones follow in accordance with the discussion in Section 2.

Finally, an exact expression for the thermal average per-site Euler characteristic in the thermodynamic limit can be calculated from (22) and (23), by noting that, in the periodic case,

$$\langle \chi \rangle = \lim_{N\to\infty} \frac{1}{N}\frac{1}{Z_P}\sum_{N_+, N_-, D} DW_P(N_+, N_-, D)a^D u^{N_+} d^{N_-}, \quad (57)$$

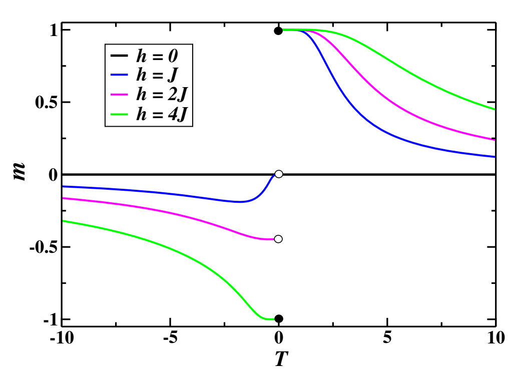

Fig. 6 (Color online) Per-site magnetization in the thermodynamic limit as a function of the temperature for the indicated magnetic fields

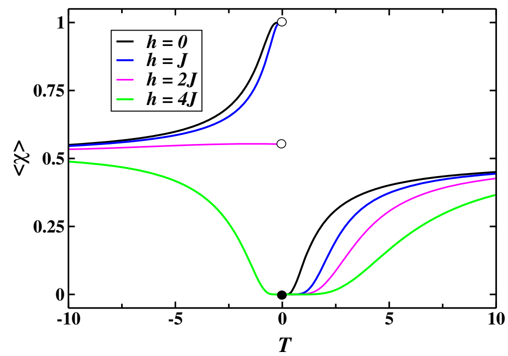

Fig. 7 (Color online) Per-site Euler characteristic in the thermodynamic limit as a function of the temperature for the indicated magnetic fields

which implies the simple relation:

$$\langle \chi \rangle = \lim_{N \to \infty} \frac{1}{N} \frac{a}{Z_P} \frac{\partial Z_P}{\partial a}. \tag{58}$$

Proper variable substitutions then lead to the result

$$\langle \chi \rangle = \frac{2e^{-2\beta J}}{\sigma_+ (\sigma_+ - \sigma_-)}. \tag{59}$$

Figure 7 shows $\langle \chi \rangle$ as a function of the temperature for various magnetic fields—only positive fields are shown, since the right-hand side of (59) is an even function of h. The plots verify the conjecture proposed in [19], since the Euler characteristic is nonvanishing for all temperatures $T > 0$, while it vanishes at the critical temperature $T_C = 0$. The loss of continuity at $T = 0$ and $|h| \leq 2J$ is easily understood if one recalls that the Euler characteristic is the average of the number of domains; indeed, at $T = 0^-$, the low-energy states are ferromagnetic, while the high-energy ones are antiferromagnetic. Interestingly, the per-site energy, Euler characteristic, and magnetization are related by the following simple relation, as it can be easily verified from (54), (56), and (59):

$$-e + 2J \langle \chi \rangle - hm = J. \tag{60}$$

4 Discussion and Closing Remarks

In this work, emphasis is given to a combinatorial topological description of the microcanonical, canonical, and grand canonical ensembles of the Ising chain in a field. From the degeneracies of the microscopic states of the system, which are discussed in detail, we compute the per-site entropy as a function of the energy under free or periodic boundary conditions. In particular, we find a residual per-site entropy for critical values of the field, a singularity for which we provided a topological interpretation and a connection with the Fibonacci sequence. We also show that in the thermodynamic limit, the logarithm of the per-site Euler characteristic is equal to the per-site entropy; in the zero field limit, moreover, the per-site Ising chain entropy is equal to the logarithm of the per-site Euler characteristic for the 1-D XY model. In addition, we identify the canonical and grand canonical partition functions with the combinatorial generating function for the microcanonical problem and provide a detailed analysis of the magnetic field dependence of the thermodynamics in the regimes of positive and negative temperatures.

We emphasize that our combinatorial approach to the canonical ensemble allows exact computation of the thermal average value of the Euler characteristic associated with the spin configurations of the chain. This topological invariant is discontinuous at the critical fields and satisfy $\langle \chi \rangle (T_C) = 0$, where $T_C = 0$ is the critical temperature, therefore confirming a conjecture in the literature. Finally, we expect that the reported results stimulate additional progress of the topological approach to phase transitions in systems exhibiting discrete symmetry and their relationship with continuous symmetry models.

Acknowledgements The authors acknowledge financial support from the Ministries of Science and Technology and Education through the funding agencies, CNPq and CAPES, and the State of Pernambuco Foundation-FACEPE.

References

1. L. Caiani, L. Casetti, C. Clementi, M. Pettini, Phys. Rev. Lett. **79**, 4361 (1997)
2. L. Casetti, E.G.D. Cohen, M. Pettini, Phys. Rev. Lett. **82**, 4160 (1999)
3. L. Casetti, E.G.D. Cohen, M. Pettini, Phys. Rev. E **65**, 036112 (2002)
4. L. Casetti, M. Pettini, E.G.D. Cohen, J. Stat. Phys. **111**, 1091 (2003)
5. R. Franzosi, M. Pettini, Phys. Rev. Lett. **92**, 060601 (2004)
6. R. Franzosi, M. Pettini, L. Spinelli, Nucl. Phys. B **782**, 189 (2007)
7. R. Franzosi, M. Pettini, Nucl. Phys. B **782**, 219 (2007)
8. M. Pettini, *Geometry and Topology in Hamiltonian Dynamics and Statistical Mechanics* (Springer, New York, 2007)
9. M. Kastner, S. Schreiber, O. Schnetz, Phys. Rev. Lett. **99**, 050601 (2007)
10. M. Kastner, O. Schnetz, Phys. Rev. Lett. **100**, 160601 (2008)
11. F.A.N. Santos, M.D. Coutinho-Filho, Phys. Rev. E **80**, 031123 (2009)
12. M. Kastner, D. Mehta, Phys. Rev. Lett. **107**, 160602 (2011)
13. J. Milnor, *Morse Theory* (Princeton University Press, Princeton, 1963)

14. Y. Matsumoto, *An Introduction to Morse Theory*, vol 208 of *Translations of Mathematical Monographs* (American Mathematical Society, Providence, 2002)
15. D. Wales, *Energy Landscapes: Applications to Clusters, Biomolecules and Glasses* (Cambridge University Press, Cambridge, 2004)
16. L. Casetti, C. Nardini, R. Nerattini, Phys. Rev. Lett. **106**, 057208 (2011)
17. C. Nardini, R. Nerattini, L. Casetti, J. Stat. Mech. Theor. Exp. **P02007**, (2012)
18. P. Blanchard, S. Fortunato, D. Gandolfo, Nucl. Phys. B **644**, 495 (2002)
19. P. Blanchard, C. Dobrovolny, D. Gandolfo, J. Ruiz, J. Stat. Mech. **03**, PO3011 (2006)
20. D. Mehta, M. Kastner, Ann. Phys. **326**, 1425 (2011)
21. M.F. Sykes, J.W. Essam, J. Math Phys. **5**, 8 (1964)
22. E. Ising, Z. Phys. **31**, 253 (1925)
23. E. Ising, *Beitrag zur Theorie des Ferro- und Paramagnetismus* (Thesis, Hamburg, 1924), (see: http://www.fhaugsburg.de/~harsch/germanica/Chronologie/20Jh/Ising/isiintr.html), in German; see also, *Special Issue: Ising Centennial Colloquium*, Bras. J. Phys. **30**(4) (2000)
24. S.I. Denisov, P. Hanggi, Phys. Rev. E **71**, 046137 (2005)
25. M. Kac, J.C. Ward, Phys. Rev. **88**, 1332 (1952)
26. T. Regge, R. Zecchina, J. Phys. A: Math. Gen. **33**, 741 (2000)
27. M. Jaric, S. Milosevic, Phys. Lett. A **48**, 367 (1974)
28. B.D. Metcalf, C.P. Yang, Phys. Rev. B **18**, 2304 (1978)
29. B.D. Stošić, T. Stošić, I.P. Fittipaldi, J.J.P. Veerman, J. Phys. A.: Math. Gen. **30**, L331 (2006)
30. S. Redner, J. Stat. Phys. **25**, 15 (1981)
31. W. Selke, M.E. Fisher, Z. Physik B **40**, 71 (1980)
32. C.S.O. Yokoi, M.D. Coutinho-Filho, S.R. Salinas, Phys. Rev. B **24**, 4047 (1981)
33. G.H. Wannier, Phys. Rev. **79**, 357 (1950)
34. G.H. Wannier, Phys. Rev. B **7**, 5017 (1973)
35. R.J. Baxter, S.K. Tsang, J. Phys. A: Math. Gen. **13**, 1023 (1980)
36. R.J. Baxter, J. Phys. A: Math. Gen. **13**, L61 (1980)
37. A.P. Ramirez, A. Hayashi, R.J. Cava, R. Siddharthan, B.S. Shastry, Nature **399**, 333 (1999)
38. S.T. Bramwell, M.J.P. Gingras, Science **294**, 1495 (2001)
39. L. Pauling, J. Am. Chem. Soc. **57**, 2680 (1935)
40. S. Sherman, J. Math. Phys. **1**, 202 (1960)
41. L. Onsager, Phys. Rev. **65**, 117 (1944)
42. R.J. Baxter, *Exactly Solved Models in Statistical Mechanics* (Academic Press, San Diego, 1989)
43. K. Huang, *Statistical Mechanics,* 2nd edn (Wiley, New York, 1987)
44. N.F. Ramsey, Phys. Rev. **103**, 20 (1956)
45. B. Stošić, S. Milošević, H.E. Stanley, Phys. Rev. B **41**, 11466 (1990)
46. C. Hwang, S. Kim, D. Kang, J.M. Kim, J. Stat. Mech. **2007**, L05001 (2007)
47. C. Vitoriano, M.D. Coutinho-Filho, E.P. Raposo, J. Phys. A: Math. Gen. **35**, 9049 (2002)
48. K.G. Wilson, J. Kogut, Phys. Rep. **12**, 75 (1974)
49. M. Polyakov, *Gauge Fields and Strings* (Harwood Academic, Chur, 1987)
50. I.P. Goulden, D.M. Jackson, *Combinatorial Enumeration* (Dover Books on Mathematics, Mineola, 1983)
51. D.R. Nelson, M.E. Fisher, Ann. Phys. **91**, 226 (1975)